ChemComm

RSC Publishing

COMMUNICATION

View Article Online
View Journal | View Issue

A novel class of polymeric pH-responsive MRI CEST agents†

Cite this: *Chem. Commun.*, 2013, **49**, 6418

Received 4th April 2013,
Accepted 26th May 2013

DOI: 10.1039/c3cc42452a

www.rsc.org/chemcomm

Shanrong Zhang,[ab] Kejin Zhou,[a] Gang Huang,[a] Masaya Takahashi,[b] A. Dean Sherry*[bc] and Jinming Gao*[ac]

In this communication, we report that ionizable, tertiary amine-based *block* copolymers can be used as pH-responsive contrast agents for magnetic resonance imaging (MRI) through the chemical exchange saturation transfer (CEST) mechanism. The CEST signal is essentially "off" when the polymers form micelles near physiological pH but is activated to the "on" state when the micelles dissociate in an acidic environment.

Balaban and coworkers first reported a new class of contrast agents for magnetic resonance imaging (MRI) based on a chemical exchange saturation transfer (CEST) mechanism.[1,2] In biological systems, many endogenous CEST agents exist either as small biomolecules or macromolecules with exchangeable –NH or –OH protons.[3–6] Exogenous CEST agents can also be designed to respond to a variety of physiological signals such as pH, temperature, enzyme activity or metabolite levels.[7–13] This new technology offers a multitude of new venues for *in vivo* molecular imaging using standard MRI scanners.

In our previous studies, we have reported a series of tertiary amine-based *block* copolymers, such as poly(ethylene glycol)-*b*-poly[2-(diisopropylamino)ethyl methacrylate] (PEG-*b*-PDPA), that form micelles at pH 7.4 and dissociate over a sharp pH range below 6.3. The micelles dissociate into unimers in acidic environments due to the switch of the amine *block* of PDPA from the hydrophobic to the hydrophilic/charged state that parallels protonation of tertiary amine groups (Scheme 1).[14,15] The pH response is sharp (ΔpH $<$ 0.25 pH units) and tunable (the transition pH, pH_t, is adjustable by changing the side chains of tertiary amines). Since the major difference between the micelle and unimer states is the protonation of tertiary amines (where the resulting ammonium groups have exchangeable protons), we anticipated that these copolymers may also serve as activatable MRI contrast agents *via* a CEST mechanism. Conceivably, the CEST signal would be silent near physiological pH (*i.e.* the micellar form does not contain exchangeable protons) but would be turned "on" in acidic environments after the micelles dissociate into protonated unimers having exchangeable protons.

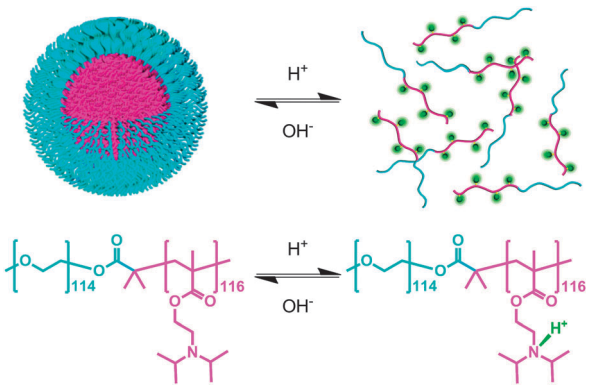

Scheme 1 The micelle–unimer equilibrium in the *block* copolymer, PEG_{114}-*b*-$PDPA_{116}$, is exquisitely sensitive to pH.

To investigate the feasibility of this approach, a PEG_{114}-*b*-$PDPA_{116}$ copolymer (114 and 116 refer to the numbers of repeating units in PEG and PDPA segments, respectively) was synthesized and used as a model system (Scheme 1 and Fig. S1 in the ESI†). Two major aspects were considered: (1) PEG-*b*-PDPA copolymers had been intensively characterized in previous studies as ultra pH-responsive fluorescent probes;[15] and (2) the pK_a of PEG-*b*-PDPA is *ca.* one pH unit below the physiological pH so that it will have large enough differences to be silent in blood yet potentially shows a CEST signal only from acidic tissues. Experimentally, the pK_a of PEG_{114}-*b*-$PDPA_{116}$ as determined by pH titration (Fig. S2 in the ESI†) was 6.27. This pK_a is 0.4 pH unit lower than that reported for a similar copolymer with a shorter $PDPA_n$ segment (n = 80) and additional

[a] *Department of Pharmacology, Harold C. Simmons Comprehensive Cancer Center, University of Texas Southwestern Medical Center, Dallas, Texas 75390, USA. E-mail: jinming.gao@utsouthwestern.edu*

[b] *Advanced Imaging Research Center, University of Texas Southwestern Medical Center, Dallas, Texas 75390, USA. E-mail: dean.sherry@utsouthwestern.edu*

[c] *Department of Chemistry, University of Texas at Dallas, Richardson, Texas 75083, USA*

† Electronic supplementary information (ESI) available: Polymer synthesis, micelle preparation, pH titration, CMC additional DLS and NMR data. See DOI: 10.1039/c3cc42452a

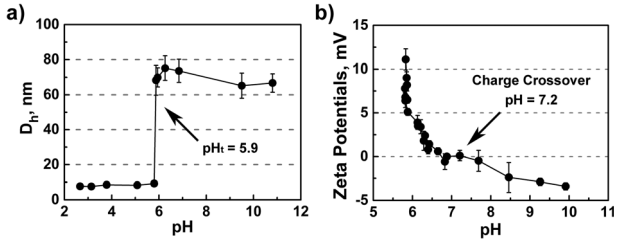

Fig. 1 (a) The hydrodynamic diameter (D_h, nm) and (b) zeta potential (mV) of PEG-*b*-PDPA as a function of pH.

fluorescent dyes (tetramethyl rhodamine).[15] In addition, the critical micelle concentration (CMC) (Fig. S3, ESI†) was found to be 0.15 μg ml^{-1} for PEG_{114}-*b*-$PDPA_{116}$, about 6-fold lower than that of PEG_{114}-*b*-$PDPA_{80}$ (CMC = 0.9 μg ml^{-1}).[15]

Fig. 1a shows the pH dependence of the hydrodynamic diameter (D_h, nm) of PEG-*b*-PDPA as measured by the dynamic light scattering (DLS). Clearly, the micelle transition occurs at a pH_t of *ca.* 5.9, about 0.4 pH units lower than that of a similar *block* copolymer with a shorter $PDPA_n$ segment (n = 80).[15] To evaluate the protonation status, the zeta potential of PEG-*b*-PDPA was also measured as a function of pH (Fig. 1b). At high pH values where the amines are de-protonated and micelles dominate, the small negative zeta potential reflects small amounts of OH^- and Cl^- anions introduced during sample preparation. As the pH is lowered, protonation (H^+) of the tertiary amines occurs and the PDPA segments acquire positive charge. It is worth noting that the charge crossover point (the point of zero charge) is approximately at pH 7.2, about one pH unit above the pK_a of the amine. In contrast, the zeta potential increases much more dramatically as the pH approaches the pH_t at ~5.9. This indicates that the protonation of the *block* copolymer is dramatically increased during the transition from micelles to unimers.

To examine the CEST feasibility of PEG-*b*-PDPA, the polymer was prepared into micelles at a polymer concentration of 0.5 mM following the published procedures.[14] The stock solution was dispersed in a 0.1 M buffer consisting of 2-(*N*-morpholino)ethanesulfonic acid (MES) and/or 3-morpholinopropane-1-sulfonic acid (MOPS) to achieve a stable pH value. The sample was ultracentrifuged using centrifuge filtration tubes with a 3 kD molecular weight cutoff (MWCO) filter. Samples of buffer alone were tested and found to have no CEST signal (Fig. S4 in the ESI†). Fig. 2a illustrates typical CEST spectra of PEG-*b*-PDPA solution at pH 5.0 and 7.5, respectively. Each data point in a CEST spectrum reflects the intensity of the solvent water signal in the ^{1}H NMR spectrum after applying a 5 s RF saturation pulse at a power level of 9.4 μT at 160 different saturation frequency offsets over the range ±20 ppm.[1,2] The negative peak at 0 ppm in these spectra reflects direct saturation of the solvent water resonance (Note: the chemical shift of bulk water was manually set to 0 ppm to better visualize the CEST peak). At pH 7.5, there is no evidence for the exchanging species that could produce CEST. At pH 5.0, however, the CEST spectrum shows quite a different lineshape, namely, an additional exchange peak appears as a shoulder at *ca.* 2–5 ppm downfield of water. This can be assigned to CEST from the exchangeable

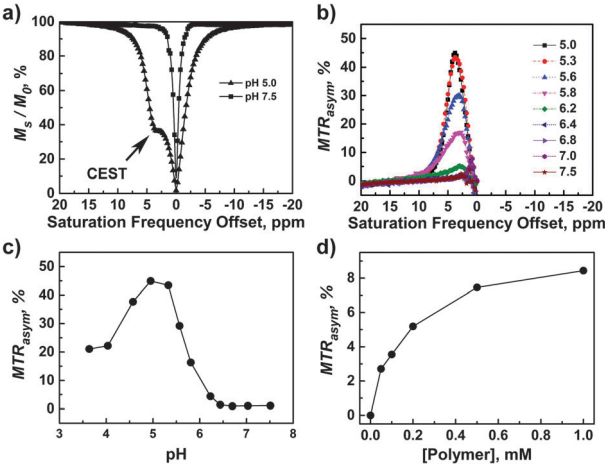

Fig. 2 (a) Representative CEST spectra of PEG-*b*-PDPA at pH 5.0 and 7.5, respectively; (b) a plot of MTR_{asym} *versus* the saturation frequency offset at the pH range between 5.0 and 7.5; (c) a plot of MTR_{asym} (±3.8 ppm) *versus* pH and (d) a plot of MTR_{asym} *versus* PEG-*b*-PDPA copolymer concentration at a fixed pH of 5.8. All data were acquired on a B_0 = 9.4 T NMR spectrometer (400 MHz for ^{1}H).

protons on the tertiary ammonium groups. Assuming that all protonated tertiary amines have an identical proton exchange rate and chemical shift, this CEST spectrum should fit well to a simple 2-pool chemical exchange model involving proton exchange between R_3N–H^+ and H_2O protons. The solid line in Fig. 2a shows the fit of the CEST data at pH 5.0 to the Bloch equations for a 2-pool model.[16] The ammonium proton lifetime (τ_{ex}) in PEG-*b*-PDPA at pH 5.0 was estimated to be ~890 μs using this fitting procedure. In addition, the corresponding monomeric analogs, *N*,*N*-diisopropylethylamine and *N*,*N*-diisopropylaminoethanol, were found to have similar CEST features (Fig. S5, ESI†). These data support the assignment of the CEST peak appearing near 2–5 ppm to the exchangeable amine proton in the polymeric form of PEG-*b*-PDPA.

The CEST effect can be better visualized in a plot of the asymmetric intensity difference between the MRI signal with presaturation at the frequency of exchanging protons (on-freq) and the MRI signal with presaturation at an equivalent frequency on the opposite side of water (off-freq),[13] *i.e.*, $MTR_{asym} = [(M_s/M_0)_{on\ freq} - (M_s/M_0)_{off\ freq}]$, as shown in Fig. 2b. For clarity, only those MTR_{asym} spectra over the pH range 5.0 to 7.5 were shown. All CEST spectra and the corresponding MTR_{asym} spectra are shown in Fig. S6 (ESI†). For PEG-*b*-PDPA, the exchanging protons are activated over a rather broad range of pH values, reaching a maximum at pH ~5. Shown in Fig. 2c is a plot of MTR_{asym} *vs.* pH for this system. There are three distinct phases in this plot: (1) the 1st phase above pH 6.5 corresponds to the non-protonated micelle state where CEST is "off"; (2) the 2nd phase between pH 5 and 6.5 shows a variable CEST "on" region where the sample is partially converted from micelles to unimers and begins to protonate; and (3) the 3rd phase below pH ~5 where proton exchange gradually becomes too slow to meet the exchange requirement for CEST. Such a bell-shaped dependence of CEST *versus* pH values was previously observed in a paramagnetic CEST system.[17] In the 1st and 2nd phases, the CEST effects present a typical switch from the totally "off"

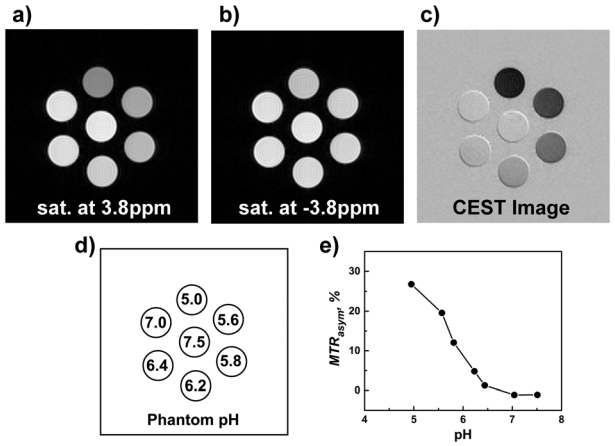

Fig. 3 9.4 T MRI images (a–c) of a phantom consisting of seven plastic tubes containing 0.5 mM PEG-*b*-PDPA solutions in the presence of 0.1 M MES–MOPS buffers at different pH values (d). The images were obtained sequentially by applying a 3 s pre-saturation pulse at either +3.8 ppm or −3.8 ppm at a power level of 8.2 μT, respectively. The CEST image (c) was obtained by image subtraction. The quantified MTR_{asym} between the images (c) and (b) were plotted in (e), which were further normalized to zero for the background.

(pH > 6.5) to gradually ''on'' (pH < 6.5). By comparing the data shown in Fig. 1b and 2c, one could conclude that the CEST effects should be proportional to the protonation percentages of the tertiary amino groups. These NMR spectroscopic data do reveal the feasibility that PEG-*b*-PDPA might be able to serve as an MRI CEST agent over a physiologically relevant pH range.

The sensitivity of detection of a contrast agent is an important parameter. Shown in Fig. 2d is a plot of MTR_{asym} *vs.* the polymer concentration at pH 5.8 (Note: this data set was acquired using a shorter saturation duration time of 3 s). This shows that an ~0.1 mM polymer is required to produce the ~3% CEST signal. This sensitivity is similar in order of magnitude to other small molecular CEST agents[1,2] or polymeric CEST agents on a per-monomer basis.[18]

To further demonstrate the feasibility of using CEST to image pH by MRI, a phantom was prepared consisting of seven plastic tubes filled with 0.5 mM PEG-*b*-PDPA solutions at different pH values (Fig. 3d). A 3 s saturation pulse (B_1 = 8.2 μT) was applied at the different frequency offsets, varying from +10 ppm to −10 ppm with a decreased step of 0.2 ppm. Shown in Fig. 3a and b are the raw images at saturation frequency offsets of +3.8 ppm and −3.8 ppm, respectively. The CEST image (Fig. 3c) was obtained *via* an image subtraction pixelwise (Fig. 3a and b). Shown in Fig. 3e is a quantified plot of MTR_{asym} (±3.8 ppm) as a function of pH. The trend has a very similar pattern to that of the spectroscopic data shown in Fig. 2c but the absolute values were different because the image intensities are related to many factors such as the MRI hardware settings, the imaging pulse sequences, *etc.*

In summary, we have shown that ionizable polymer-based CEST probes may be used as pH-responsive MRI CEST agents. This system is unique in that CEST is essentially ''off'' at normal physiological pH and only switched ''on'' in an acidic environment. This pH-activatable micelle platform may find useful applications for *in vivo* MRI molecular imaging of acidosis-related metabolic diseases as well as for monitoring the pH-responsive drug delivery using pH-responsive micelles as nanocarriers.

This research was supported by grants from the National Institutes of Health to JG (CA129011 and EB013149) and ADS (CA-115531, EB-004582 and EB-015908).

Notes and references

1 K. M. Ward, A. H. Aletras and R. S. Balaban, *J. Magn. Reson.*, 2000, **143**, 79–87.
2 K. M. Ward and R. S. Balaban, *Magn. Reson. Med.*, 2000, **44**, 799–802.
3 J. Zhou, J. F. Payen, D. A. Wilson, R. J. Traystman and P. C. M. van Zijl, *Nat. Med.*, 2003, **9**, 1085–1090.
4 J. Zhou and P. C. M. van Zijl, *Prog. Nucl. Magn. Reson. Spectrosc.*, 2006, **48**, 109–136.
5 A. A. Gilad, M. T. McMahon, P. Walczak, P. T. Winnard, V. Raman, H. W. M. van Laarhoven, C. M. Skoglund, J. W. M. Bulte and P. C. M. van Zijl, *Nat. Biotechnol.*, 2007, **25**, 217–219.
6 K. Cai, M. Haris, A. Singh, F. Kogan, J. H. Greenberg, H. Hariharan, J. A. Detre and R. Reddy, *Nat. Med.*, 2012, **18**, 302–306.
7 S. Zhang, M. Merritt, D. E. Woessner, R. E. Lenkinski and A. D. Sherry, *Acc. Chem. Res.*, 2003, **36**, 783–790.
8 S. Aime, S. Crich, E. Gianolio, G. Giovenzana, L. Tei and E. Terreno, *Coord. Chem. Rev.*, 2006, **250**, 1562–1579.
9 M. Woods, D. E. Woessner and A. D. Sherry, *Chem. Soc. Rev.*, 2006, **35**, 500–511.
10 S. Aime, D. D. Castelli, S. G. Crich, E. Gianolio and E. Terreno, *Acc. Chem. Res.*, 2009, **42**, 822–831.
11 M. M. Ali, G. Liu, T. Shah, C. A. Flask and M. D. Pagel, *Acc. Chem. Res.*, 2009, **42**, 915–924.
12 L. M. De Leon-Rodriguez, A. J. M. Lubag, C. R. Malloy, G. V. Martinez, R. J. Gillies and A. D. Sherry, *Acc. Chem. Res.*, 2009, **42**, 948–957.
13 P. C. M. van Zijl and N. N. Yadav, *Magn. Reson. Med.*, 2011, **65**, 927–948.
14 K. Zhou, Y. Wang, X. Huang, K. Luby-Phelps, B. D. Sumer and J. Gao, *Angew. Chem., Int. Ed.*, 2011, **50**, 6109–6114.
15 K. Zhou, H. Liu, S. Zhang, X. Huang, Y. Wang, G. Huang, B. D. Sumer and J. Gao, *J. Am. Chem. Soc.*, 2012, **134**, 7803–7811.
16 D. E. Woessner, S. Zhang, M. E. Merritt and A. D. Sherry, *Magn. Reson. Med.*, 2005, **53**, 790–799.
17 S. Zhang and A. D. Sherry, *International Society for Magnetic Resonance in Medicine, 10th Scientific Meeting & Exhibition*, Honolulu, Hawaii, United States, 2002, p. 2590.
18 N. Goffeney, J. W. M. Bulte, J. Duyn, L. H. Bryant and P. C. M. van Zijl, *J. Am. Chem. Soc.*, 2001, **123**, 8628–8629.

